Solid-oxide fuel cells (SOFC) with hydrocarbon and hydrocarbon-derived fuels

Colorado School of Mines | California Institute of Technology

Robert J. Kee and Huayang Zhu
Engineering Division, Colorado School of Mines
Golden, CO 80401, USA

David G. Goodwin
Engineering and Applied Science, California Institute of Technology
Pasadena, CA 91125, USA

rjkee@mines.edu
(303) 273-3379

Presented:
International Symposium on Combustion
July 29, 2004

Direct-oxidation fuel cells offer a number of potentially important benefits

Colorado School of Mines | California Institute of Technology

Direct conversion to electricity (hydrocarbon fuels and syngas)
High efficiency at relatively low temperature (~ 700°C)
- Combined cycles (heat engines and combined heat-power)

Eliminate high-temperature moving parts (reliable and quiet)
Extremely low emissions

But, there is much research and development to be done
- Fundamental understanding of charge-transfer electrochemistry
- Fuel pyrolysis and deposit formation
- Reforming and partial oxidation processes (catalysis)
- System design and optimization, including balance of plant
- Many materials issues (electrodes, electrolyte, seals, interconnect,...)

Important intersections with combustion science and technology
- Fundamental chemistry, theory and diagnostics
- Hybrid cycles, including combustion of partially spent fuels
- Chemically reacting flow generally

There is important fuel-cell physics and chemistry spanning a great range of scales

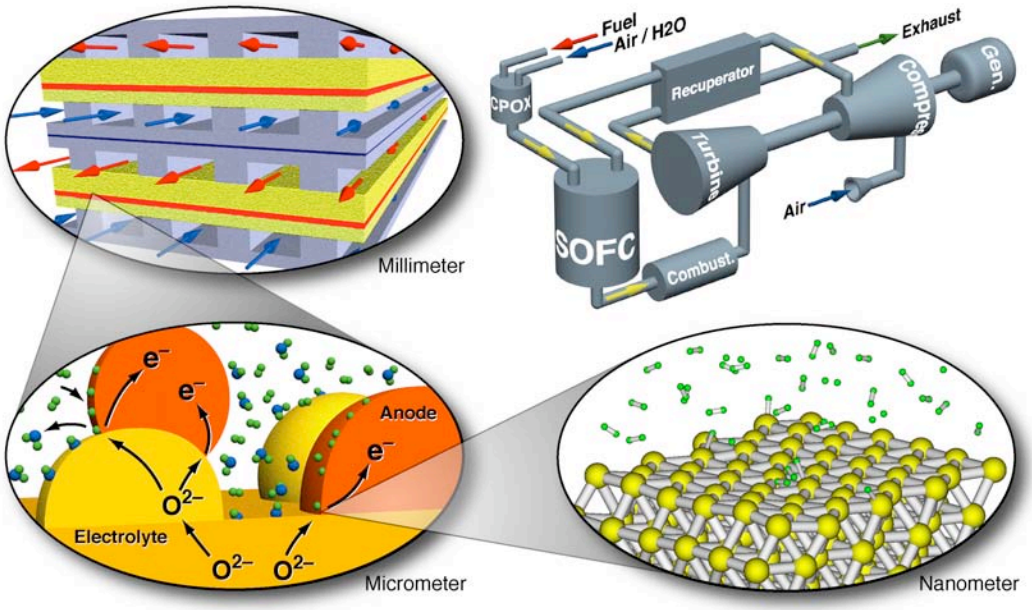

There is an extensive and growing literature in fuel cells generally and SOFC particularly

General SOFC resources

- "The Fuel Cell Handbook," US Dept. of Energy, 6th Ed., DOE/NETL 2002/1179, available on the web, (2002).
- Singhal and Kendall, "High-temperature SOFC," Elsevier, (2003).
- Minh and Takahashi, "Science and Technology of Ceramic Fuel Cells," Elsevier, (1995).

Seminal research on hydrocarbon-fueled SOFC

- E. Perry Murray, T. Tsai, and S.A. Barnett, "A direct-methane fuel cell with a ceria-based anode," *Nature*, 400:651-659 (1999)
- S. Park, J.M. Vohs, and R.J. Gorte, "Direct oxidation of hydrocarbons in a solid-oxide fuel cell," *Nature*, 404: 265-266 (2000)

Broad areas of research and literature

- Materials (electrolyte, electrodes, catalysts, interconnects, seals,…)
- Membrane-electrode assemblies
- Fuel cell characterization and performance
- Fundamental electrochemical processes
- Systems and hybrid cycles

Solid-Oxide Fuel Cells enable direct electro-chemical oxidation (DECO) of hydrocarbons

Colorado School of Mines — California Institute of Technology

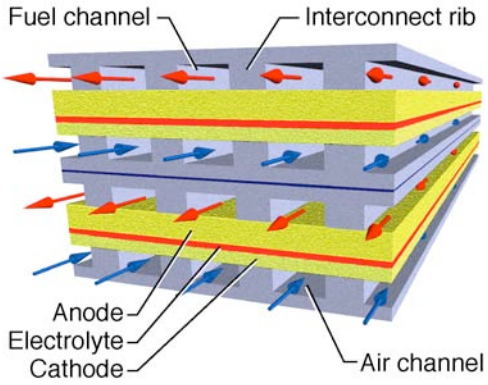

Characteristic dimension: 1 mm
- Channel diameter
- Anode thickness

Characteristic temperature: 700˚C

Planar architecture
- Membrane-electrode assembly
- Interconnect carries current
- Stacked layers build voltage

Electrolyte (e.g., YSZ)
- Polycrystalline ceramic
- O^{2-} ion conductor
- Electrical insulator
- Impervious to gas flow

Electrodes
- Porous cermet composite
- Anode supports MEA

Interconnect
- High electrical conductivity
- Maintains equal potential

Flow channels
- Formed in interconnect

Fuel-cell operation depends on coupled macroscopic and microscopic processes

Colorado School of Mines — California Institute of Technology

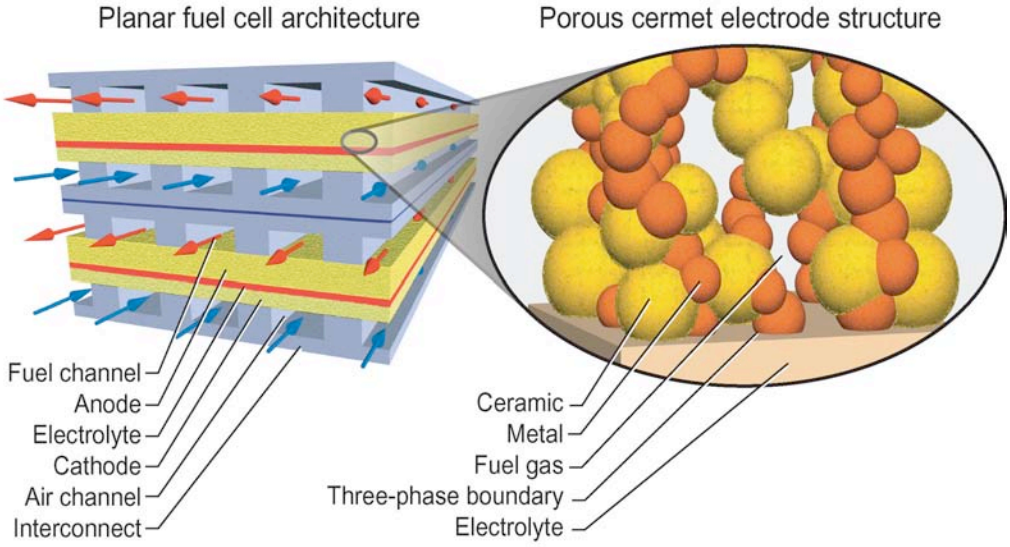

There are similarities and differences between PEM and SOFC technology

Proton Exchange Membrane (PEM)
- Polymer electrolyte
- Proton-conducting electrolyte
- Low temperature (~100˚C)
- Requires H2 fuel
- CO is a poison
- Needs good reforming/separation
- Precious-metal catalysts
- Low thermal inertia
- Fairly mature

Solid Oxide Fuel Cell (SOFC)
- Ceramic electrolyte
- Oxygen-ion conductor
- High temperature (~700˚C)
- Can use hydrocarbon fuel
- CO is not a poison
- May use reforming or CPOX
- Inexpensive catalysts
- Large thermal inertia
- In development

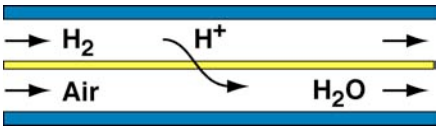

PEM

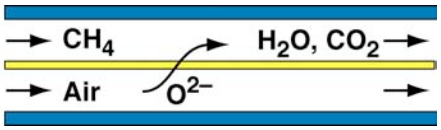

SOFC

Experiments to characterize and evaluate new material systems are often done with small “button cells”

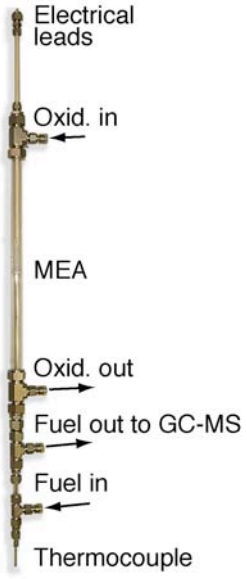

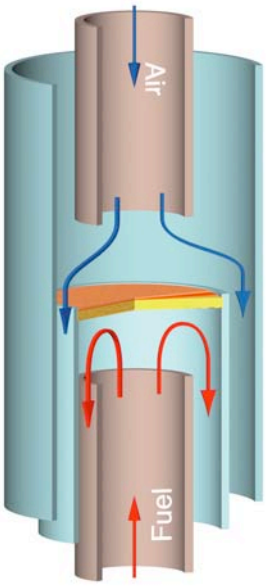

From the laboratory of Prof. Sossina Haile, Caltech

Direct electrochemical oxidation has been demonstrated for a variety of fuels

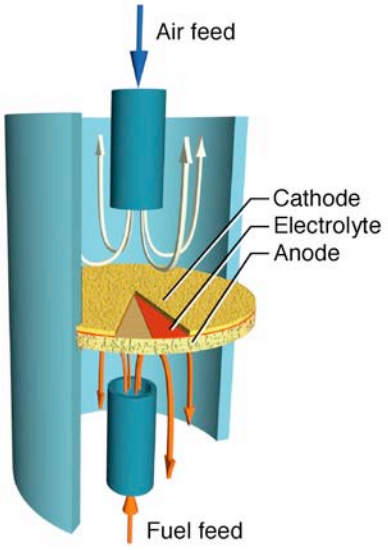

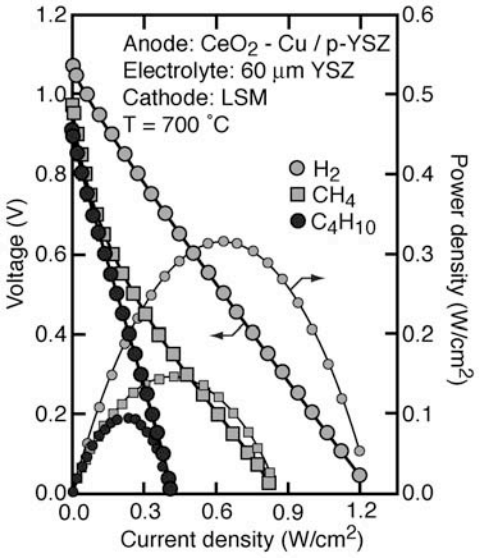

Data: Gorte, Kim, and Vohs,
J. Power Sources, 106:10-15 (2002)

A practical SOFC needs extensive three-phase boundaries to facilitate charge transfer

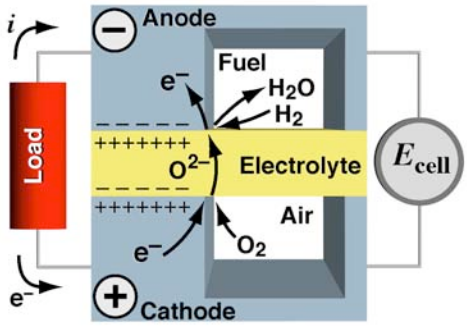

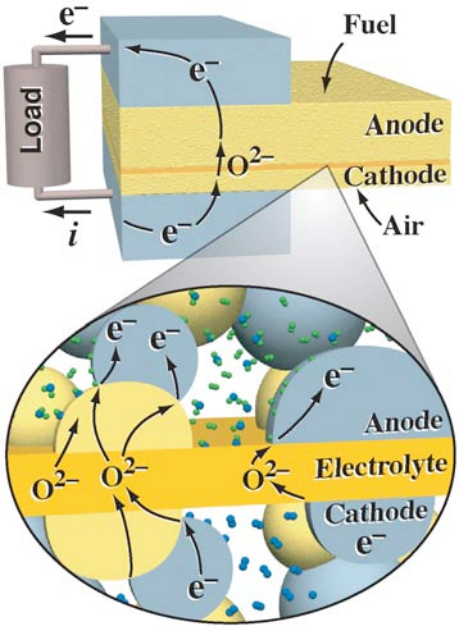

Cathode charge transfer:

$$O_2(g) + 4e^-(c) \rightleftharpoons 2O^{2-}(el)$$

Anode charge transfer:

$$H_2(g) + O^{2-}(el) \rightleftharpoons H_2O(g) + 2e^-(a)$$

Net:

$$H_2(g) + \tfrac{1}{2}O_2(g) \rightleftharpoons H_2O(g)$$

There is a long and expanding set of materials that are being developed for fuel-cell applications

Colorado School of Mines | California Institute of Technology

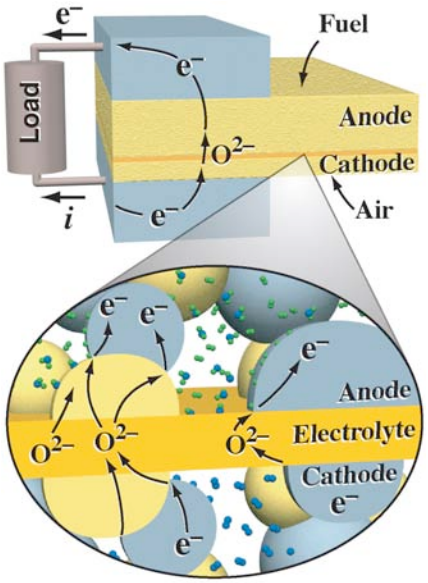

Interconnect
- Metals (Fe-Cr alloys)
- Ceramics (e.g., $LaCrO_3$)

Electrolyte
- Yttria-stabilized zirconia, YSZ
- Samarium doped ceria, SDC
- Gadolinium doped ceria, GDC

Cathode
- Mixed ionic-electronic conductors
  - Doped (e.g., Sr) $LaMnO_3$, LSM
  - $La_{1-x}Sr_xCo_{1-y}Fe_yO_{3-\delta}$, LSCF
- Cermets

Anode
- Cermets (e.g., Ni-YSZ, Ni-SDC)
- Ceria-copper

Membrane-electrode assemblies (MEA) can be fabricated by tape-casting or extrusion technologies

Colorado School of Mines | California Institute of Technology

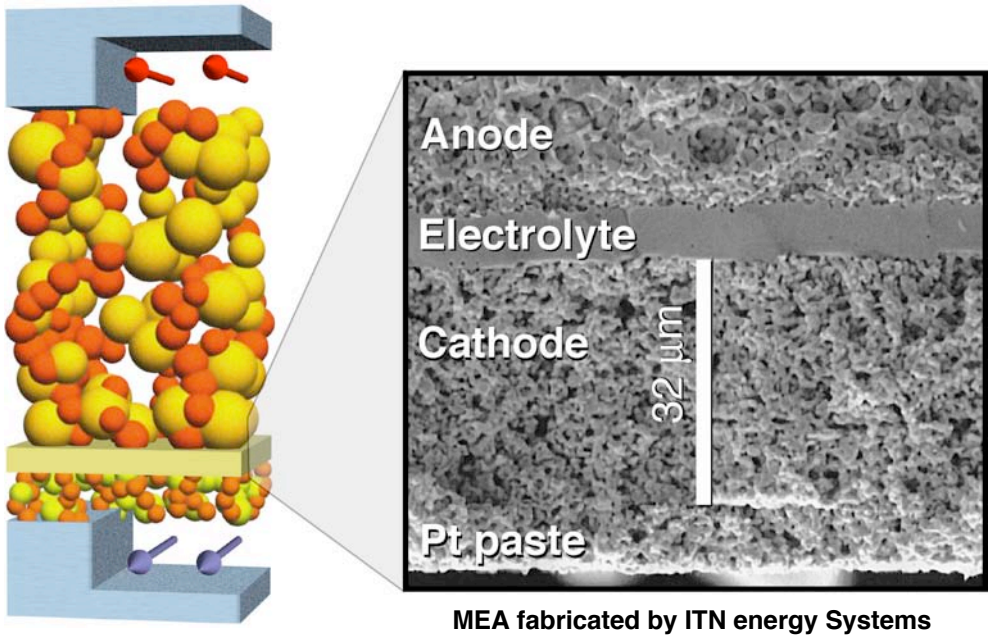

MEA fabricated by ITN energy Systems

At equilibrium the electric potentials are related to the chemical potentials of the fuel and oxidizer streams

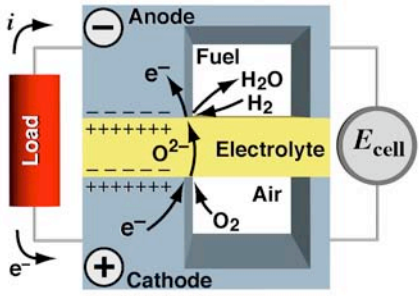

Cathode charge transfer:

$O_2(g) + 4e^-(c) \rightleftharpoons 2O^{2-}(el)$

Anode charge transfer:

$H_2(g) + O^{2-}(el) \rightleftharpoons H_2O(g) + 2e^-(a)$

Net:

$H_2(g) + \frac{1}{2}O_2(g) \rightleftharpoons H_2O(g)$

For reversible reactions at equilibrium

$$\sum_k \nu_k \tilde{\mu}_k = 0$$

Electrochemical and chemical potentials

$$\tilde{\mu}_k = \mu_k + z_k F \phi_k$$

Cathode charge exchange

$$\mu_{O_2,c} - 4F\phi_c = 2\mu_{O^{2-},c} - 4F\phi_{e,c}$$

Cathode-electrolyte potential difference:

$$E_c = \phi_c - \phi_{e,c} = (1/4F)(\mu_{O_2} - 2\mu_{O^{2-},c})$$

Similarly, at the anode

$$\mu_{H_2} + \mu_{O^{2-},a} - 2F\phi_{e,a} = \mu_{H_2O} - 2F\phi_a$$

$$E_a = (1/2F)(\mu_{H_2O} - \mu_{O^{2-},a} - \mu_{H_2})$$

Reversible cell potential

$$E_{rev} = E_c - E_a = \frac{1}{2F}\left[\mu_{H_2} + \frac{1}{2}\mu_{O_2} - \mu_{H_2O}\right]$$

Reversible cell potential is determined entirely from thermodynamics of the gas streams

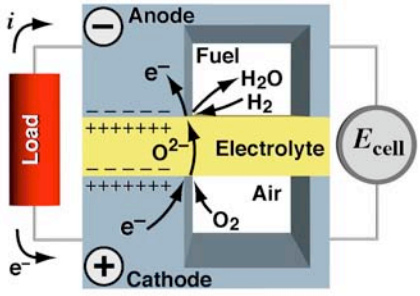

Cathode charge transfer:

$O_2(g) + 4e^-(c) \rightleftharpoons 2O^{2-}(el)$

Anode charge transfer:

$H_2(g) + O^{2-}(el) \rightleftharpoons H_2O(g) + 2e^-(a)$

Net:

$H_2(g) + \frac{1}{2}O_2(g) \rightleftharpoons H_2O(g)$

Reversible cell potential

$$E_{rev} = E_c - E_a = \frac{1}{2F}\left[\mu_{H_2} + \frac{1}{2}\mu_{O_2} - \mu_{H_2O}\right]$$

where $\tilde{\mu}_{O^{2-},a} = \tilde{\mu}_{O^{2-},c}$ at equilibrium

For ideal gases

$$\mu_k = \mu_k^\circ + RT \ln p_k$$

$$\Delta G^\circ = \mu^\circ_{H_2O} - \mu^\circ_{H_2} - \frac{1}{2}\mu^\circ_{O_2}$$

$$E_{rev} = -\frac{\Delta G^\circ}{2F} + \frac{RT}{2F} \ln \frac{p_{H_2} p_{O_2}^{1/2}}{p_{H_2O}}$$

The electrical potential of the cell depends on the fuel type and fuel dilution

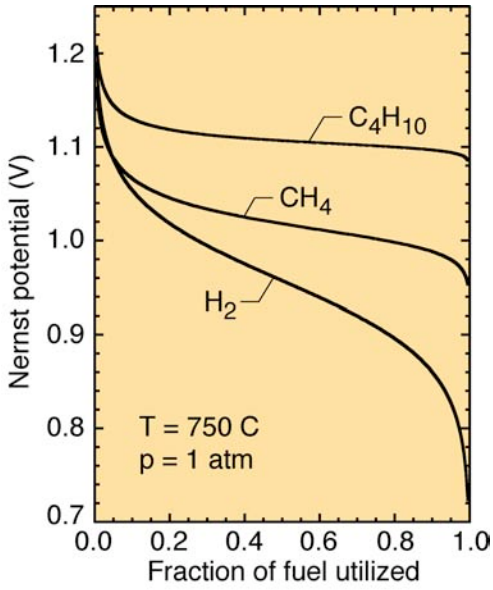

Assuming direct oxidation

C_4H_{10} + (13/2) O_2 -> 5 H_2O + 4 CO_2

CH_4 + 2 O_2 -> 2 H_2O + CO_2

H_2 + (1/2) O_2 -> H_2O

Global oxidation reaction

$$CH_4 + 2O_2 \rightleftharpoons 2H_2O + CO_2$$

Reversible thermodynamic efficiency

$$\varepsilon_{t,rev} = \frac{\Delta G}{\Delta H} = \frac{\Delta G^\circ}{\Delta H^\circ} + \frac{RT}{\Delta H^\circ} \ln \prod_k p_k^{\nu_k} \approx 90\%$$

$$\varepsilon_{carnot} = 1 - \frac{T}{T_o} < 90\%$$

Acheived efficiency

$$\varepsilon = \frac{W_{elec}}{\dot{m}(h_{in} - h_{ox})} = \frac{\int E_{cell} i(x) dx}{\dot{m}(h_{in} - h_{ox})} \approx 50\%$$

Thermodynamic and Utilization efficiency

$$\varepsilon = \varepsilon_t \varepsilon_f$$

$$\varepsilon_t = \frac{W_{elec}}{W_{elec} + Q} = \frac{W_{elec}}{\dot{m}(h_{in} - h_{out})}$$

$$\varepsilon_f = \frac{(h_{in} - h_{out})}{(h_{in} - h_{ox})}$$

Irreversible losses, fuel depletion, and fuel utilization serve to reduce fuel-cell efficiency

Cell performance depends on the chemical potential of fuel and oxidizer and on internal losses

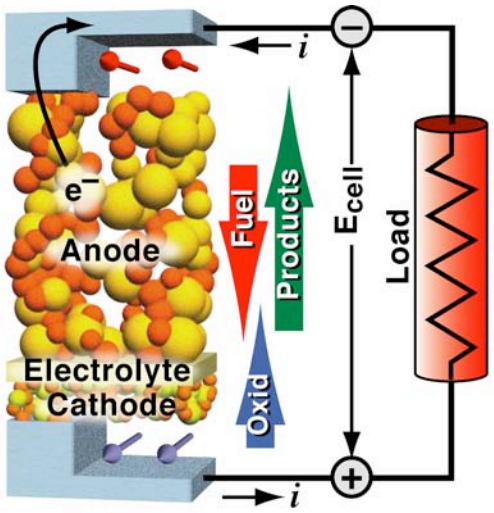

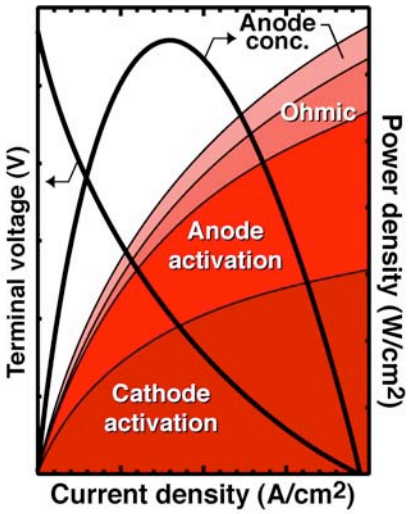

The ohmic overpotential through the electrolyte depends greatly on temperature

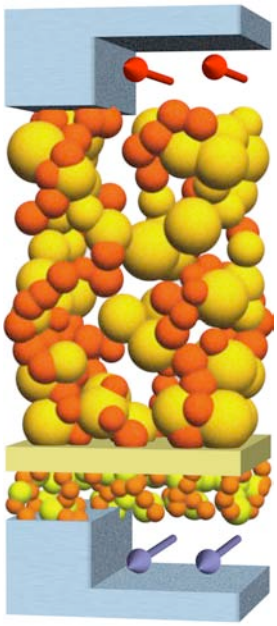

Ohmic overpotential

$$\eta_{\text{ohm}} = iR_{\text{el}}$$

Electrolyte resistance

$$R_{\text{el}} = \frac{L_{\text{el}}}{\sigma_{\text{el}}}$$

Electrolyte ion conductivity

$$\sigma_{\text{el}} = \sigma_0 T^{-1} \exp\left(-\frac{E_{\text{el}}}{RT}\right)$$

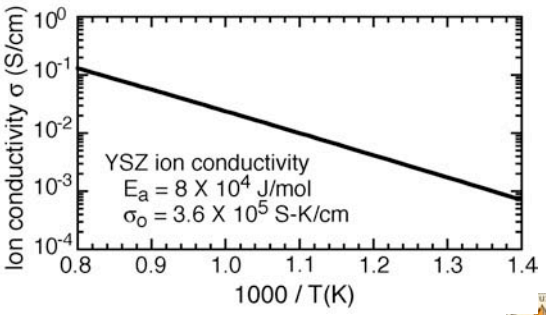

Activation overpotentials represent the chemical energy needed to overcome charge-transfer barriers

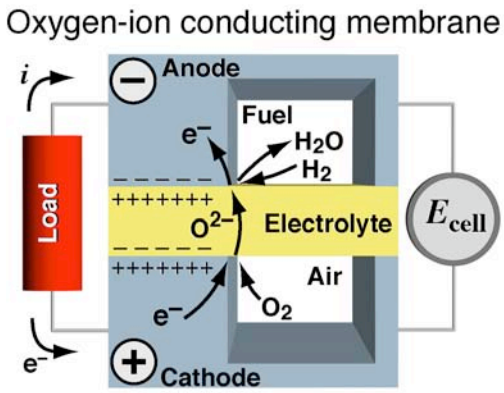

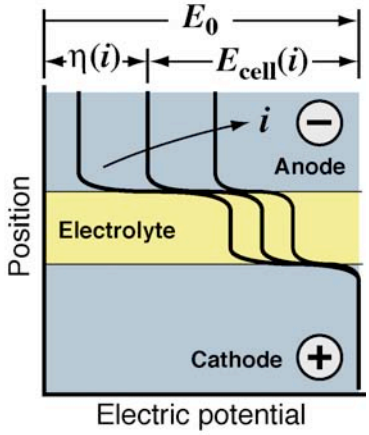

Overpotential $\eta(i)$ is relative to the equilibrium potential: $E_{\text{cell}} = E_{\text{eq}} - \eta$

Exchange current density is at equilibrium potential: $i_0 = i_f = i_r$

Butler-Volmer equation:

$$i = i_f - i_r = i_0 \left[\exp\left(\frac{\alpha F \eta}{RT}\right) - \exp\left(-\frac{(1-\alpha)F\eta}{RT}\right) \right]; \; i_0 = i_0^0(T) \prod_{k=1}^{K} [X_k]^{\gamma_k}$$

There is great uncertainty in the details of elementary charge-transfer chemical reaction mechanisms

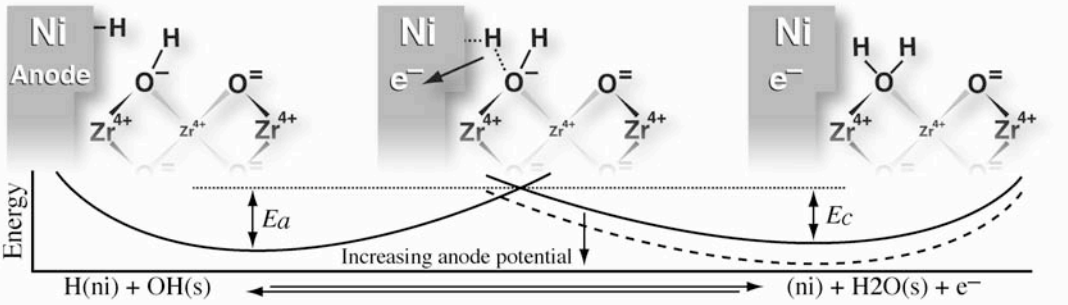

Nickel surface reactions

H_2 + (ni) + (ni) <=> H(ni) + H(ni)

H_2O + (ni) + (ni) <=> OH(ni) + H(ni)

OH(ni) + H(ni) <=> O(ni) + H_2 + (ni)

Triple-phase charge exchange

H(ni) + O(s) <=> (ni) + e^- + OH(s)

H(ni) + OH(s) <=> (ni) + H_2O(s) + e^-

YSZ surface reactions

VO(s) + Ox <=> VO + O(s)

H_2O(s) <=> H_2O + VO(s)

Surface and bulk species

(ni)	Empty Ni site
H(ni)	H adsorbed on Ni
OH(ni)	OH adsorbed on Ni
Ox	Bulk oxygen ion, charge = –2
VO	Bulk oxygen vacancy
VO(s)	Oxygen vacancy on YSZ
O(s)	Surface O ion, charge = –2
H_2O(s)	Surface H_2O
OH(s)	Surface OH, charge = –1

The electric-potential bias affects the activation barriers to charge-transfer

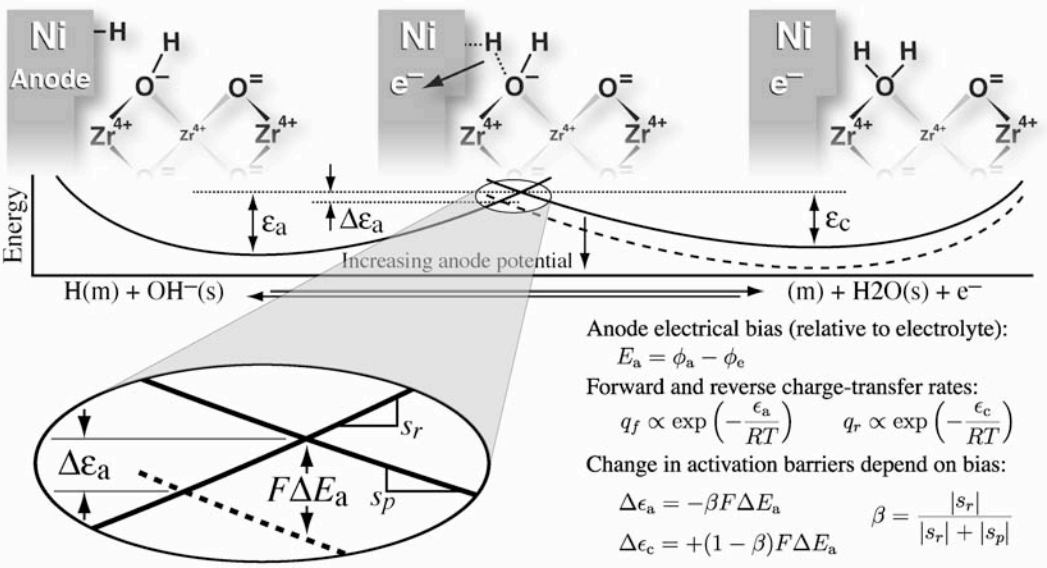

Anode electrical bias (relative to electrolyte):

$$E_a = \phi_a - \phi_e$$

Forward and reverse charge-transfer rates:

$$q_f \propto \exp\left(-\frac{\epsilon_a}{RT}\right) \qquad q_r \propto \exp\left(-\frac{\epsilon_c}{RT}\right)$$

Change in activation barriers depend on bias:

$$\Delta\epsilon_a = -\beta F \Delta E_a \qquad \beta = \frac{|s_r|}{|s_r| + |s_p|}$$

$$\Delta\epsilon_c = +(1-\beta) F \Delta E_a$$

The Butler-Volmer form of the charge-transfer rates can be derived from mass-action concepts

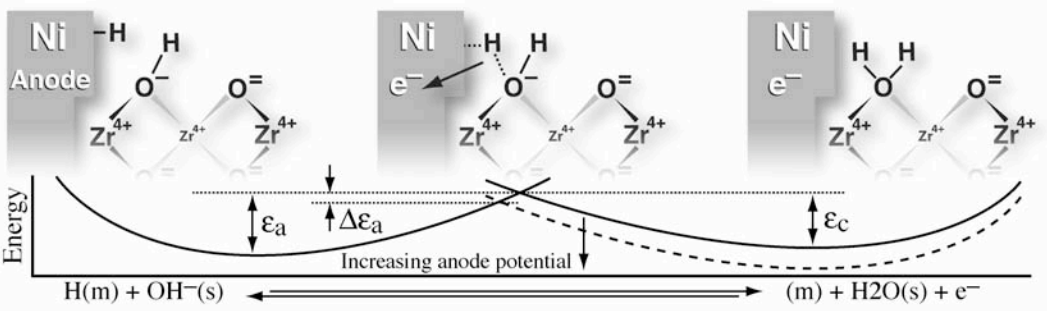

Rate of progress:

$$q = L_{tpb}\left[k_a(T)\theta_H\theta_{OH}e^{\beta F E_a/RT} - k_c(T)\theta_m\theta_w e^{-(1-\beta)FE_a/RT}\right]$$

Thermal rate constants and coverages:

$$k_a(T), \quad k_c(T), \quad \theta_H, \quad \theta_{OH}, \quad \theta_m, \quad \theta_w$$

Microscopic reversibility at $E_a = 0$:

$$k_a(T)/k_c(T) = K_p(T) = \exp(-\Delta G^\circ/RT)$$

Equilibrium electric potential:

$$E_{a,eq} = \frac{\Delta G^\circ(T)}{F} - \frac{RT}{F}\ln\left(\frac{\theta_H\theta_{OH}}{\theta_m\theta_w}\right)$$

Define overpotential: $\eta \equiv E_a - E_{a,eq}$

Current density in Butler-Volmer form:

$$i = i_0\left[e^{\beta F\eta/RT} - e^{-(1-\beta)F\eta/RT}\right]$$

Exchange current density:

$$i_0 = F L_{tpb} k_a e^{\beta\Delta G^\circ(T)/RT}\left(\theta_H\theta_{OH}\right)^{1-\beta}\left(\theta_w\theta_m\right)^{\beta}$$

Butler-Volmer reaction orders are different from elementary orders

- **Electric-potential difference versus Overpotential**

Estimates of adsorption, desorption, and diffusion assist estimating the extent of the three-phase regions

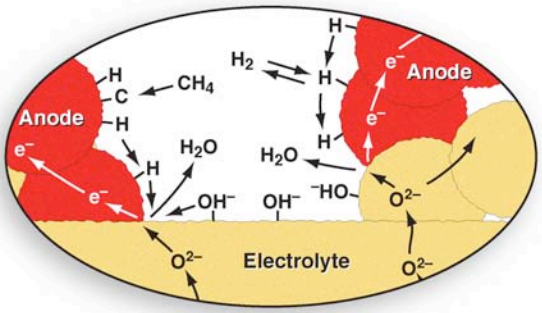

Hydrogen adsorption/desorption on Ni

$$H_2 + 2(\mathrm{Ni}) \rightleftharpoons 2\mathrm{H(Ni)}$$

Adsorption sticking probability: $\gamma \approx 0.1$

Desorption rate: $q_d \approx n_0 \nu_\mathrm{d} \exp(-E_\mathrm{d}/RT)\theta_\mathrm{H}^2$

Steady-state H coverage (700°C):

$$\theta_\mathrm{H} = \frac{(p_{\mathrm{H}_2}/p^*)^{1/2}}{1+(p_{\mathrm{H}_2}/p^*)^{1/2}} \approx 0.45$$

Mean lifetime of chemisorbed H (700°C):

$$\tau_\mathrm{H} = \frac{\exp(E_\mathrm{d}/RT)}{\nu_\mathrm{d}\theta_\mathrm{H}} \approx 12\ \mathrm{ns}$$

Diffusion of H on Ni:

$$D_\mathrm{H} \approx 0.0025 \exp(-1762/T)\ \mathrm{cm^2/s}$$

Diffusion length scale (700°C):

$$\ell_\mathrm{d} \approx \sqrt{D_\mathrm{H}\tau_\mathrm{H}} \approx 20\ \mathrm{nm}$$

Most adsorbed H does not participate in charge transfer

- **Benefits to making nano-dispersed electrodes**

To what extent are parallel charge-exchange pathways coupled ?

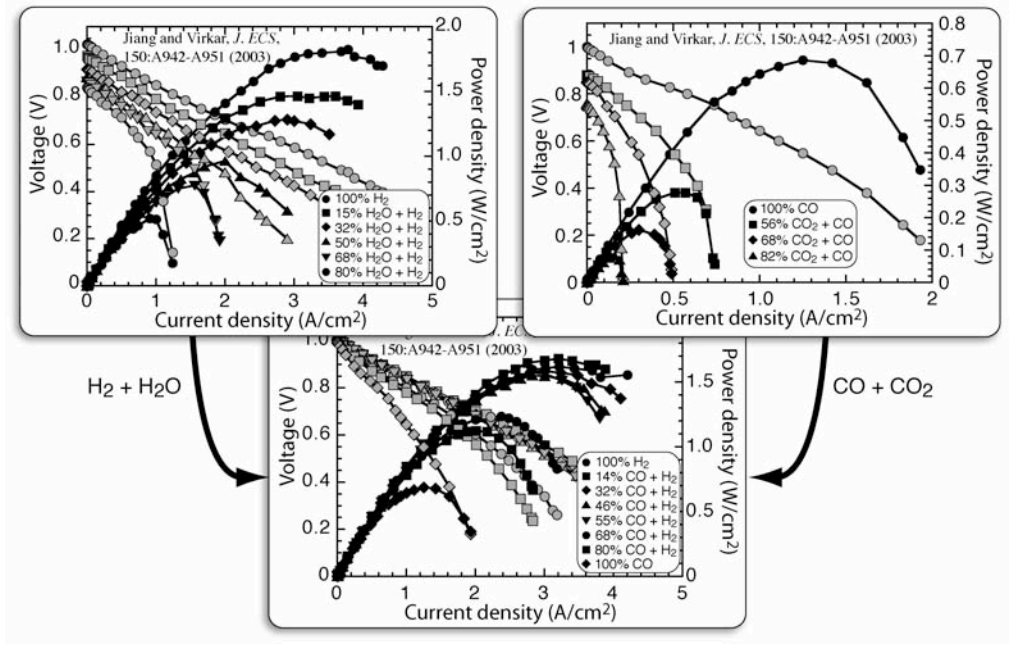

Pattern anodes can expose chemical processes that are obscured from observation in a fuel cell

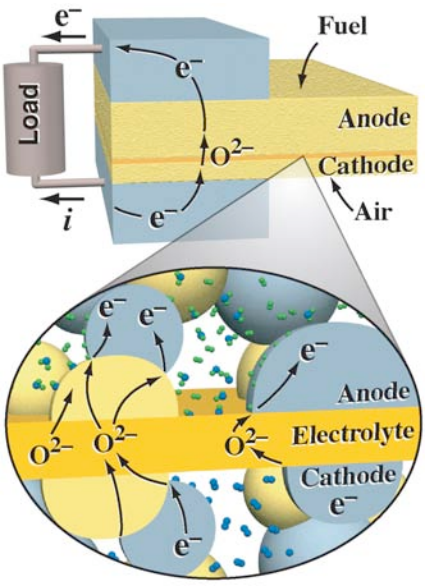

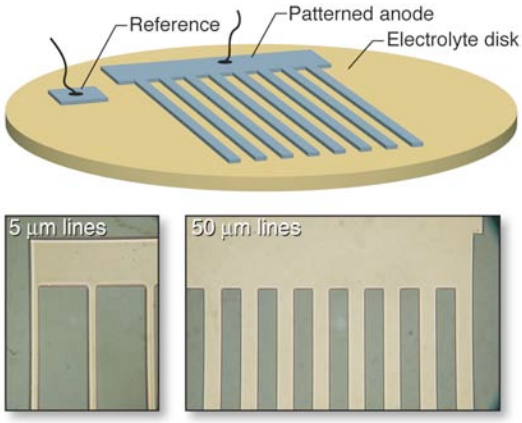

Pattern anode SEM images courtesy of Profs. G. Jackson, R. Walker, and B. Eichhorn, University of Maryland

Microfabrication technology is used to make well defined three-phase boundaries

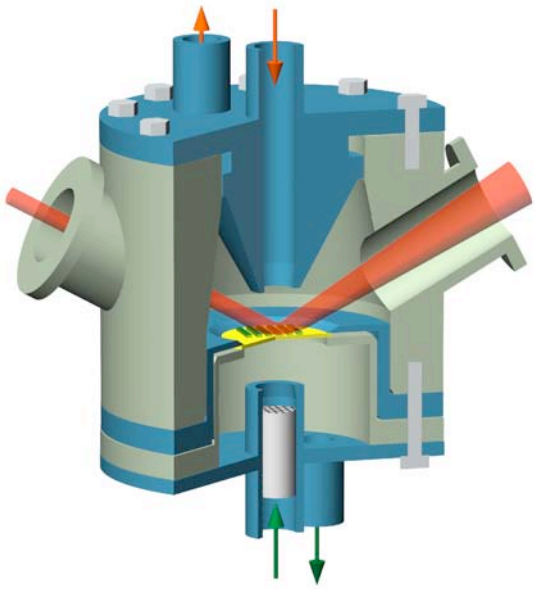

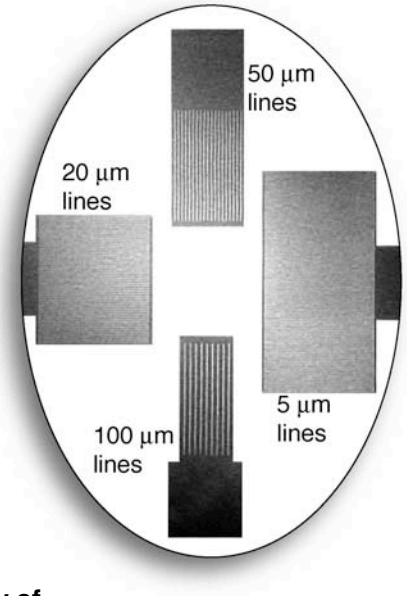

From the laboratory of Profs. G. Jackson, R. Walker, and B. Eichhorn (University of Maryland)

Patterned-anode models assist interpreting experimental electrochemical observations

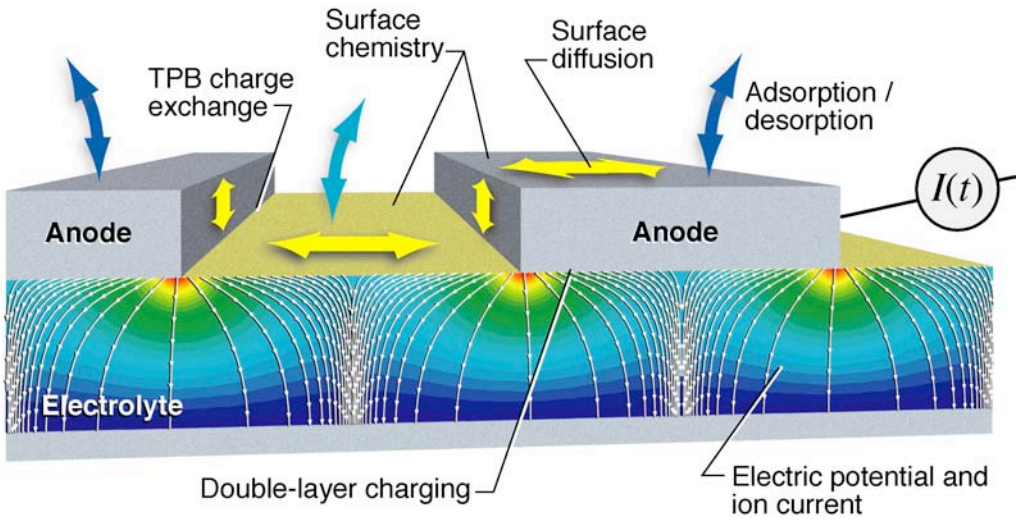

Current-dependent losses (overpotentials) reduce the actual cell voltage during operation

$$E_{\text{cell}} = E - \eta_{\text{conc,a}} - \eta_{\text{act,a}} - \eta_{\text{ohm}} - \eta_{\text{conc,c}} - \eta_{\text{act,c}} - \eta_{\text{interface}} - \eta_{\text{leakage}}$$

Concentration overpotentials
- Species transport through electrodes

Activation overpotentials
- Electrochemistry at TPB

Ohmic overpotential
- Resistive losses in electrolyte

Interface overpotentials
- Resistance at materials interfaces

Leakage overpotential
- Electrical conduction in electrolyte

The Dusty-Gas model considers that the mean-free path length is comparable to the pore size

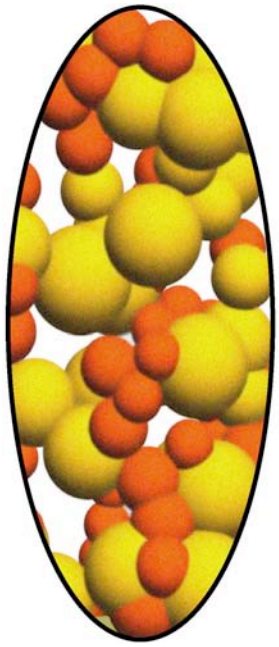

Dusty-gas model

$$\sum_{\ell \neq k} \frac{[X_\ell]\mathbf{J}_k - [X_k]\mathbf{J}_\ell}{[X_T]D^{\mathrm{e}}_{k\ell}} + \frac{\mathbf{J}_k}{D^{\mathrm{e}}_{k,\mathrm{Kn}}} = -\nabla[X_k] - \frac{[X_k]}{D^{\mathrm{e}}_{k,\mathrm{Kn}}}\frac{B_{\mathrm{g}}}{\mu}\nabla p$$

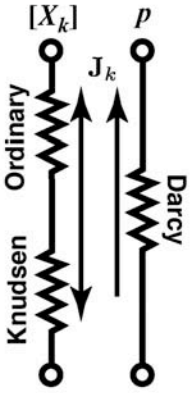

Effective Binary and Knudsen diffusion

$$D^{\mathrm{e}}_{k\ell} = \frac{\phi_{\mathrm{g}}}{\tau_{\mathrm{g}}} D_{k\ell} \qquad D^{\mathrm{e}}_{k,\mathrm{Kn}} = \frac{4}{3}\frac{r_p \phi_{\mathrm{g}}}{\tau_{\mathrm{g}}}\sqrt{\frac{8RT}{\pi W_k}}$$

Permeability (Kozeny-Carman)

$$B_{\mathrm{g}} = \frac{\phi_{\mathrm{g}}^3 d_p^2}{72\tau_{\mathrm{g}}\left(1-\phi_{\mathrm{g}}\right)^2}$$

$\mathbf{J}_k$	Molar flux	ϕ_{g}	Porosity
$[X_k]$	Concentration	τ_{g}	Tortuosity
		r_p	Pore radius
p	Pressure	d_p	Particle diameter

What is the role of the anode structure in promoting reforming, shifting, and CPOX?

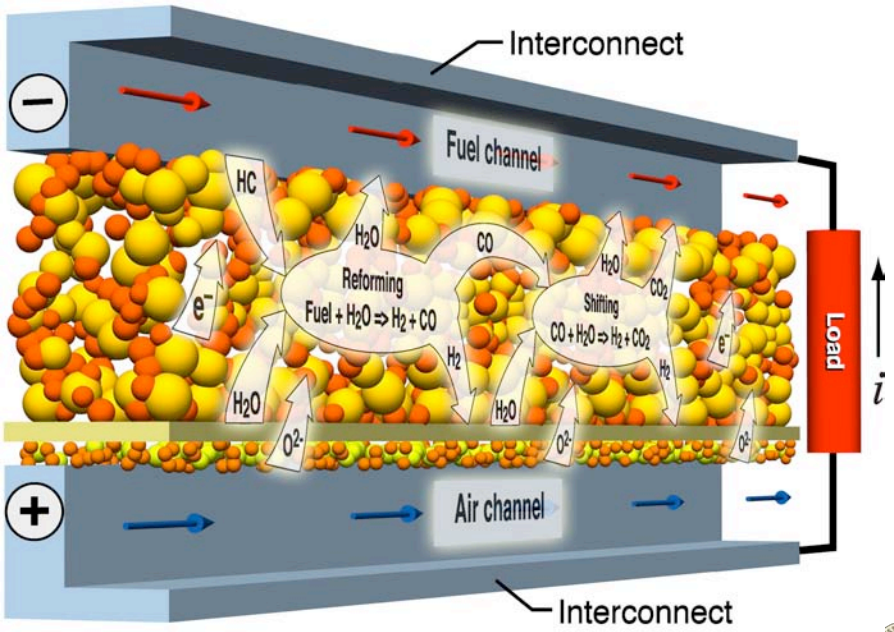

The models are capable of handling elementary heterogeneous reforming/CPOX chemistry

	Reaction	A^*	E_a^*
Adsorption:			
1.	$H_2 + Ni(s) + Ni(s) \rightarrow H(s) + H(s)$	$1.000 \cdot 10^{-2\dagger}$	0.0
2.	$O_2 + Ni(s) + Ni(s) \rightarrow O(s) + O(s)$	$1.000 \cdot 10^{-2\dagger}$	0.0
3.	$CH_4 + Ni(s) \rightarrow CH_4(s)$	$8.000 \cdot 10^{-3\dagger}$	0.0
4.	$H_2O + Ni(s) \rightarrow H_2O(s)$	$1.000 \cdot 10^{-1\dagger}$	0.0
5.	$CO_2 + Ni(s) \rightarrow CO_2(s)$	$1.000 \cdot 10^{-5\dagger}$	0.0
Desorption:			
6.	$CO + Ni(s) \rightarrow CO(s)$	$5.000 \cdot 10^{-1\dagger}$	0.0
7.	$H(s) + H(s) \rightarrow Ni(s) + Ni(s) + H_2$	$3.000 \cdot 10^{21}$	98.0
8.	$O(s) + O(s) \rightarrow Ni(s) + Ni(s) + O_2$	$1.300 \cdot 10^{22}$	464.0
9.	$H_2O(s) \rightarrow H_2O + Ni(s)$	$6.000 \cdot 10^{13}$	68.9
10.	$CO(s) \rightarrow CO + Ni(s)$	$1.000 \cdot 10^{13}$	122.4
		$\theta_{CO(s)}$	-50.0
11.	$CO_2(s) \rightarrow CO_2 + Ni(s)$	$1.000 \cdot 10^{8}$	27.3
12.	$CH_4(s) \rightarrow CH_4 + Ni(s)$	$2.000 \cdot 10^{14}$	25.1
13.	$H(s) + O(s) \rightarrow OH(s) + Ni(s)$	$5.000 \cdot 10^{22}$	97.9
Surface reaction:			
14.	$OH(s) + Ni(s) \rightarrow H(s) + O(s)$	$3.000 \cdot 10^{20}$	34.3
15.	$H(s) + OH(s) \rightarrow H_2O(s) + Ni(s)$	$3.000 \cdot 10^{20}$	42.7
16.	$H_2O(s) + Ni(s) \rightarrow H(s) + OH(s)$	$3.000 \cdot 10^{22}$	87.0
17.	$OH(s) + OH(s) \rightarrow H_2O(s) + O(s)$	$3.000 \cdot 10^{21}$	100.0
18.	$H_2O(s) + O(s) \rightarrow OH(s) + OH(s)$	$3.000 \cdot 10^{21}$	207.5
19.	$C(s) + O(s) \rightarrow CO(s) + Ni(s)$	$5.200 \cdot 10^{23}$	148.1
20.	$CO(s) + Ni(s) \rightarrow C(s) + O(s)$	$2.500 \cdot 10^{21}$	139.7
		$\theta_{CO(s)}$	-50.0
21.	$CO(s) + O(s) \rightarrow CO_2(s) + Ni(s)$	$2.000 \cdot 10^{20}$	123.6

	$(s) \rightarrow CO(s) + O(s)$	$3.000 \cdot 10^{23}$	88.0
	$(s) \rightarrow CH_3(s) + H(s)$	$3.700 \cdot 10^{21}$	57.7
	$s) \rightarrow CH_4(s) + Ni(s)$	$3.700 \cdot 10^{21}$	56.1
	$(s) \rightarrow CH_2(s) + H(s)$	$3.700 \cdot 10^{24}$	100.0
	$s) \rightarrow CH_3(s) + Ni(s)$	$3.700 \cdot 10^{21}$	49.8
	$(s) \rightarrow CH(s) + H(s)$	$3.700 \cdot 10^{24}$	97.1
	$) \rightarrow CH_2(s) + Ni(s)$	$3.700 \cdot 10^{24}$	73.6
	$s) \rightarrow C(s) + H(s)$	$3.700 \cdot 10^{21}$	18.8
	$\rightarrow CH(s) + Ni(s)$	$3.700 \cdot 10^{21}$	173.6
	$s) \rightarrow CH_3(s) + OH(s)$	$1.700 \cdot 10^{24}$	88.3
	$H(s) \rightarrow CH_4(s) + O(s)$	$3.700 \cdot 10^{21}$	23.4
	$s) \rightarrow CH_2(s) + OH(s)$	$3.700 \cdot 10^{24}$	130.1
	$H(s) \rightarrow CH_3(s) + O(s)$	$3.700 \cdot 10^{21}$	16.7
	$s) \rightarrow CH(s) + OH(s)$	$3.700 \cdot 10^{24}$	126.8
	$(s) \rightarrow CH_2(s) + O(s)$	$3.700 \cdot 10^{21}$	40.2
	$) \rightarrow C(s) + OH(s)$	$3.700 \cdot 10^{21}$	48.1
	$) \rightarrow CH(s) + O(s)$	$3.700 \cdot 10^{21}$	139.7
	$) \rightarrow HCO(s) + Ni(s)$	$5.000 \cdot 10^{19}$	96.2
	$i(s) \rightarrow CO(s) + H(s)$	$3.700 \cdot 10^{21}$	0.0
		$\theta_{CO(s)}$	50.0
	$i(s) \rightarrow CH(s) + O(s)$	$3.700 \cdot 10^{24}$	95.8
	$) \rightarrow HCO(s) + Ni(s)$	$3.700 \cdot 10^{21}$	146.0

ers for the rate constants written in the form:
$_a/RT$). The units of A are given in terms of moles,
conds. E_a is in kJ/mol.
ions 20 and 41, -0.97 for reactions 22 and 39.
.
ge (e.g., $\theta_{CO(s)}$) is specified as a site fraction.
ce site density is $\Gamma = 2.60 \times 10^{-9}$ mol/cm^2.

Reaction mechanism from Prof. Olaf Deutschmann, University of Karlsruhe

MEA models do a good job of representing measured electrochemical performance

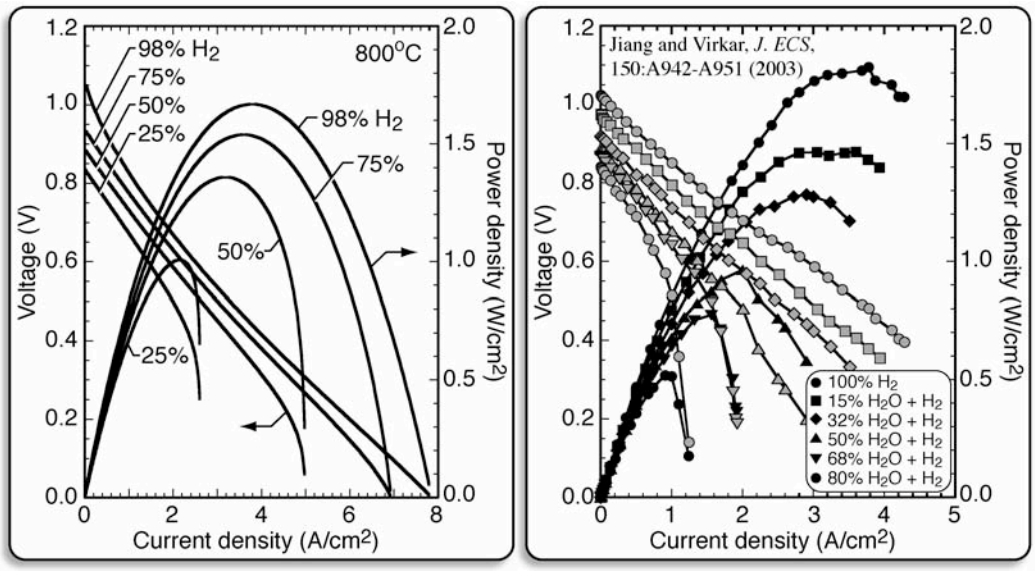

Channel models couple flow, porous transport, chemistry, and electrochemistry

Colorado School of Mines | California Institute of Technology

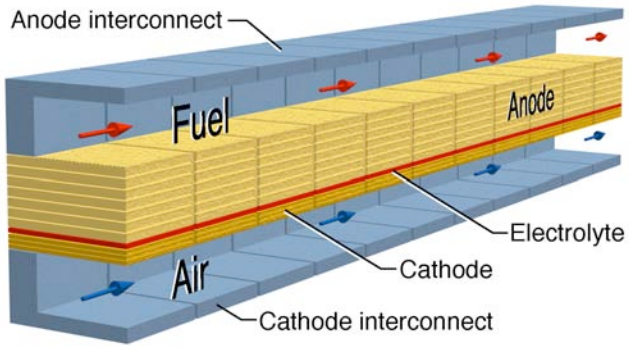

Channel flow
- Plug flow is usually appropriate
- Mass exchange with anode

Anode transport and chemistry
- Gas and surface species
- Porous-media transport
- Elementary surface chemistry

Electrochemistry
- Charge transfer rates
- **Ion transport**

Finite-volume discretization
- Computational solution

With appropriate catalysts, there can be significant reforming within the anodes

Colorado School of Mines | California Institute of Technology

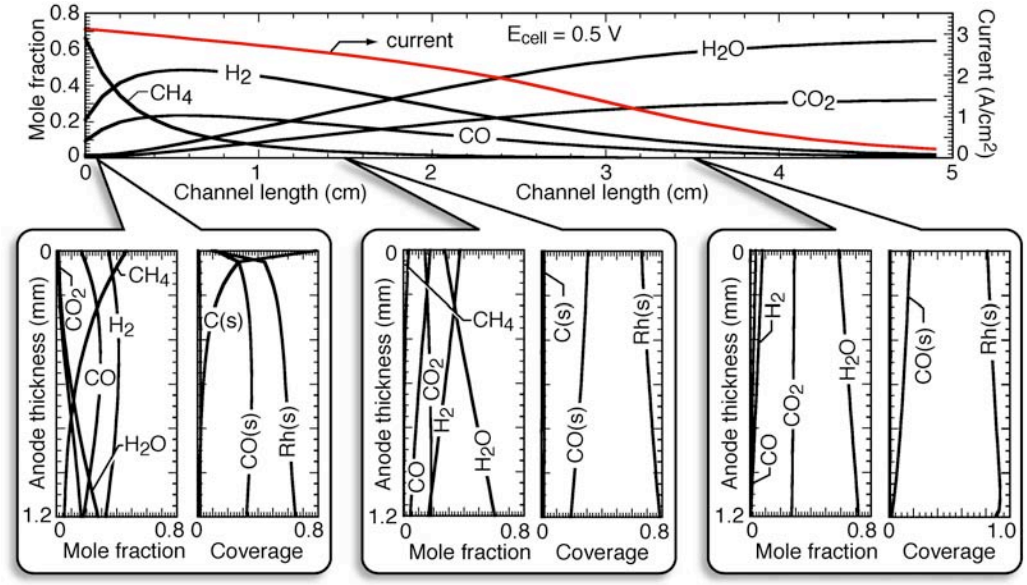

Anode Inlet: 97% CH_4, 3% H_2O, 12.5 cm/s, 800˚C, 1 atm.
Cathode: Air

The local voltage-current characteristics of the MEA vary along the channel because of fuel dilution

Colorado School of Mines | California Institute of Technology

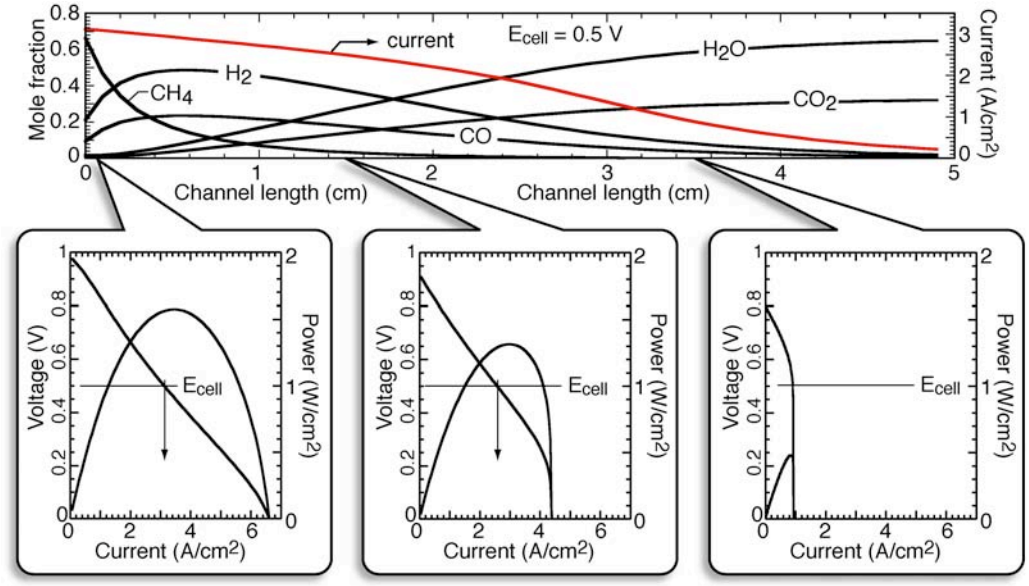

Anode Inlet: 97% CH_4, 3% H_2O, 12.5 cm/s, 800˚C, 1 atm.
Cathode: Air

Homogeneous chemistry models predict fuel conversion and deposits

Colorado School of Mines | California Institute of Technology

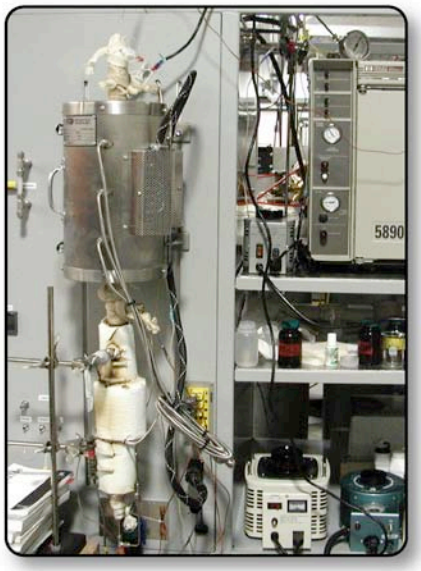

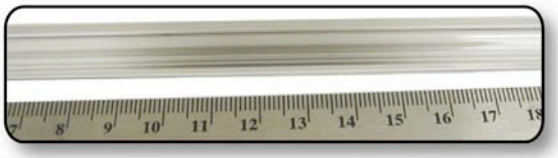

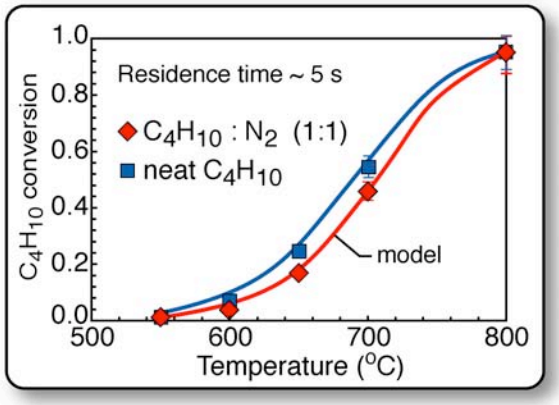

From the laboratory of Prof. A.M. Dean (Colorado School of Mines)

Homogeneous fuel pyrolysis can lead to the formation of polyaromatic deposits

Colorado School of Mines | California Institute of Technology

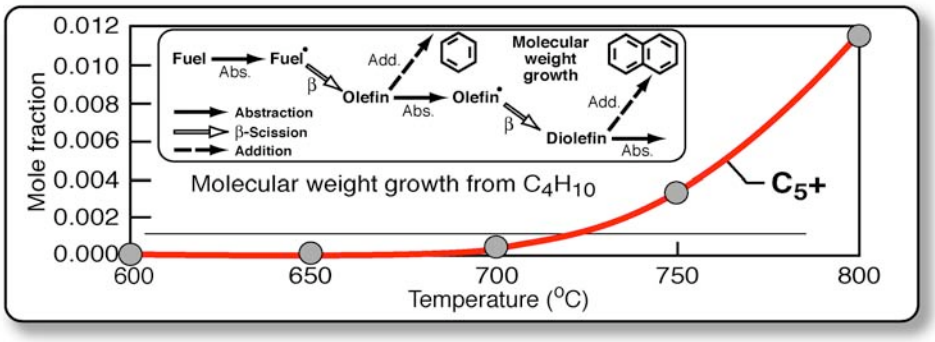

- Initial steps lead to production of smaller unsaturated species
  - Results from hydrogen-abstraction, β-scission sequences
- Molecular weight growth (deposit formation) occurs at later times
  - As unsaturates concentrations increase, radical-addition reactions become more important
  - As resonantly-stabilized radical concentrations increase, recombination reactions become important

Upstream fuel processing can help to reduce coking and fouling

Colorado School of Mines | California Institute of Technology

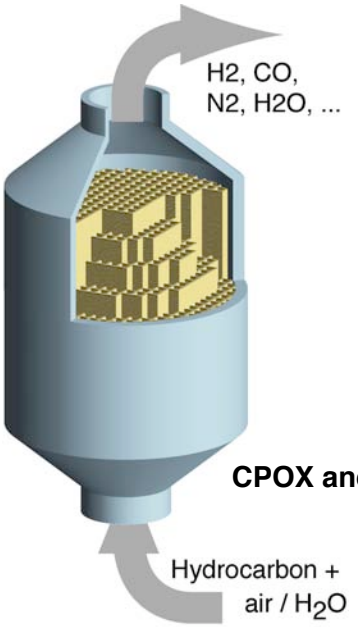

CPOX and/or Reform

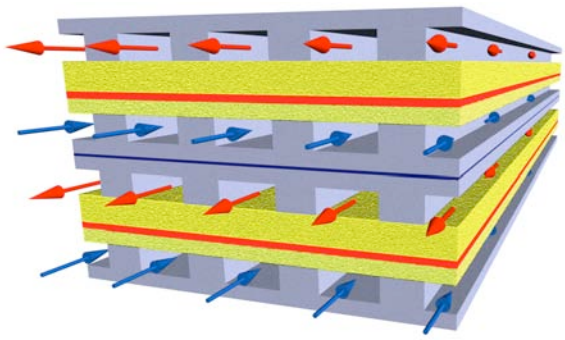

Improved fuel-cell function
- Increase H_2 content
- Reduce coking

Recently reported results provide strong evidence for internal CPOX

Colorado School of Mines — California Institute of Technology

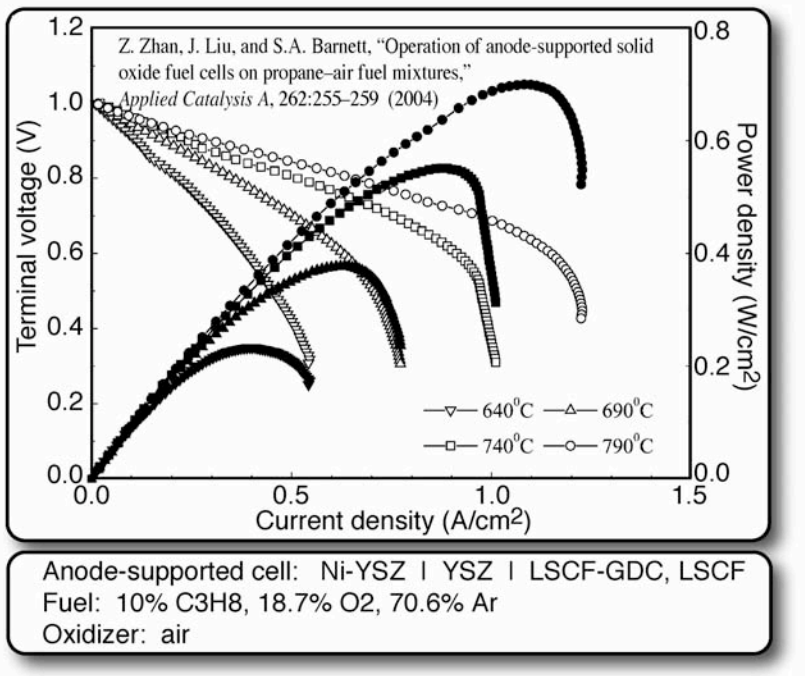

Small SOFC systems can operate with clean kerosene fuel

Colorado School of Mines — California Institute of Technology

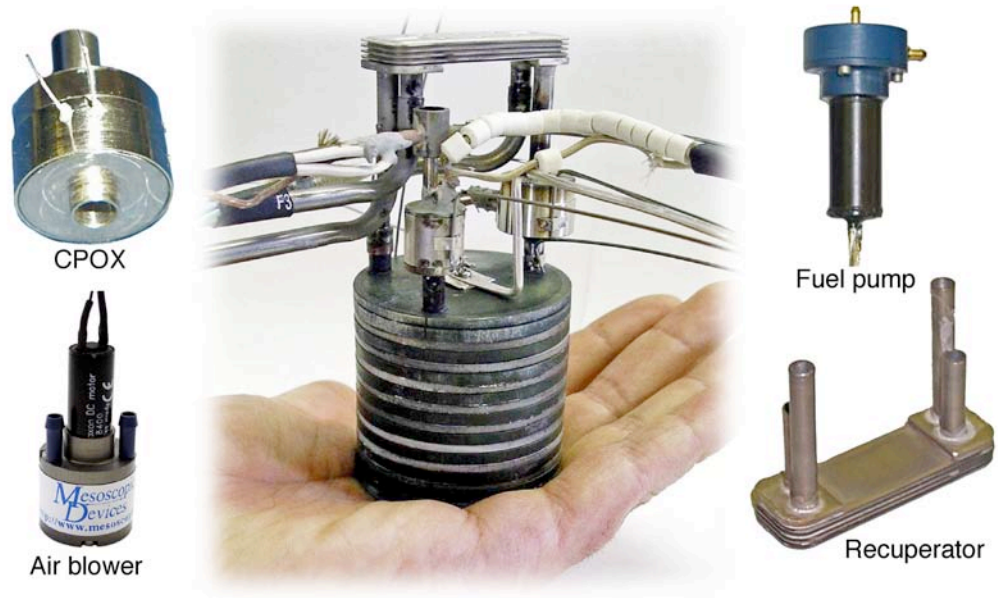

20 Watt system designed and built by ITN Energy Systems, Inc. and Mesoscopic Devices, Inc.

There are several tubular configurations that offer alternatives to planar systems

Colorado School of Mines | California Institute of Technology

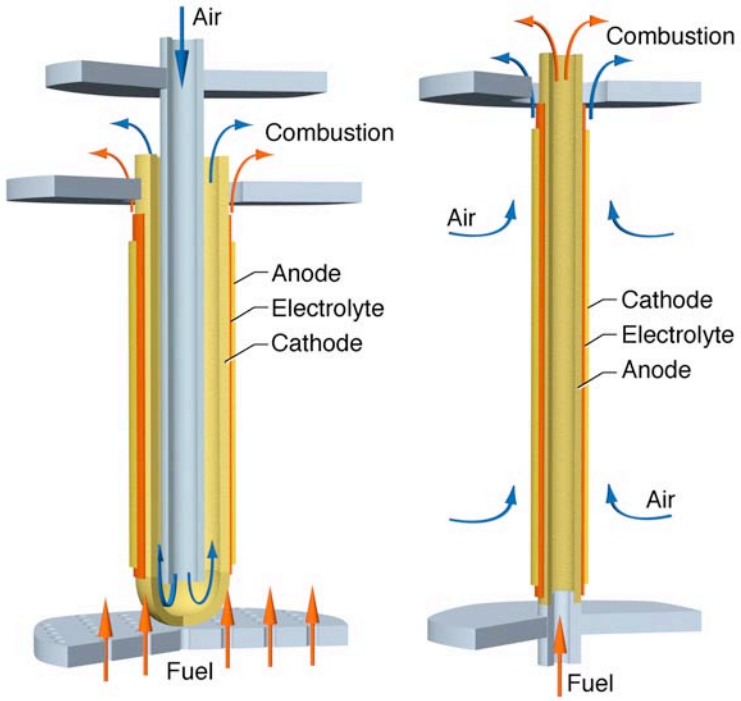

Hybrid cycles can offer overall system efficiencies of over 70%

Colorado School of Mines | California Institute of Technology

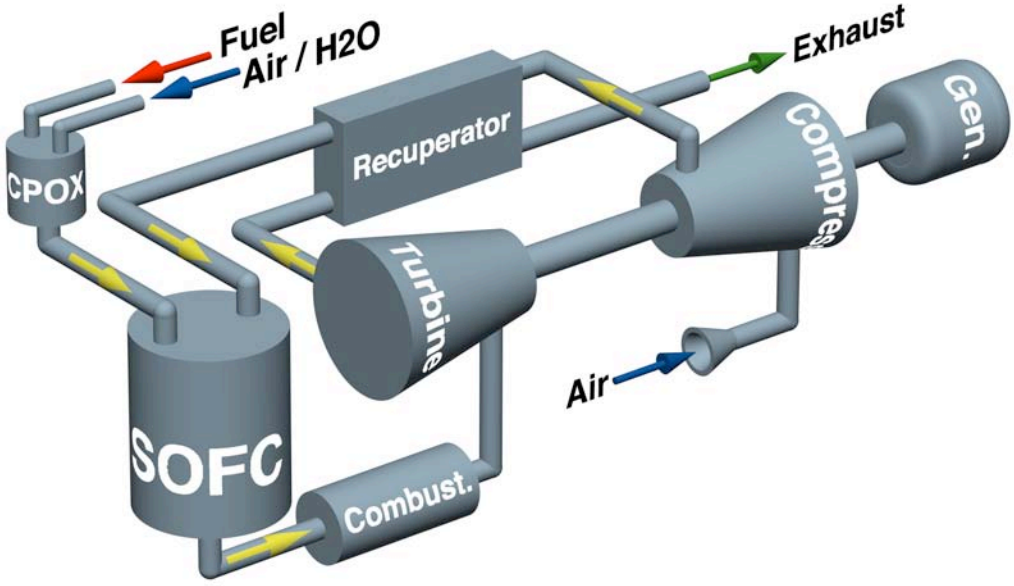

Biomass gasification and SOFC can be integrated into a hybrid system

System layout adapted from
Dr. Nikhil Patel, EERC,
Univ.of North Dakota

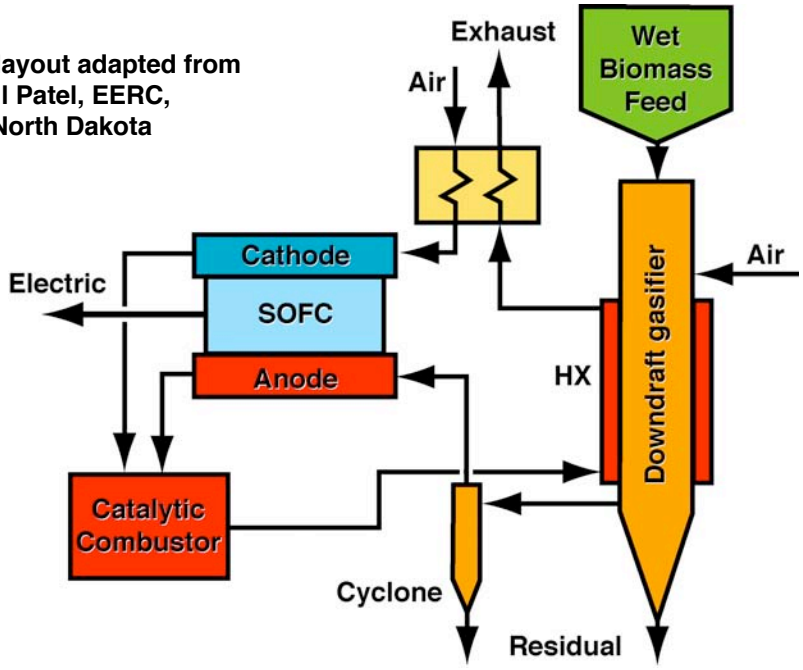

There are a great many research opportunities

Elementary electrochemical kinetics mechanisms and formalism
- Charge-transfer processes and kinetics
- Transport by surface diffusion, including field effects
- Local three-phase boundary geometry
- Selective heterogeneous and catalytic reactions
- Thermal and electrochemical competitions (e.g., H on surface)

Coking propensity and deposit formation
- Influence of catalysts, including functionally graded systems
- Influence of temperature, residence time, fuel mixes, etc.

In-situ fuel-altering processes in channels and porous electrodes
- Partial oxidation and reforming
- Functionally graded materials

Hybrid systems
- Heat engines or Combined heat and power
- Biofuels

Many materials issues

Acknowledgements

Office of Naval Research MURI
- CSM (Kee, Lusk, and Dean)
- Caltech (Goodwin, Haile, and Goddard)
- University of Maryland (Jackson, Walker, and Eichhorn)

DARPA (Palm Power)
- ITN Energy Systems (Barker, Sullivan, and Thoen)

Review and Comments on Manuscript
- Olaf Deutschmann (Karlsruhe)
- Greg Jackson (Maryland)
- Tony Dean (CSM)